*Design, Development, and Applications of Structural Ceramics, Composites, and Nanomateriah.*
Edited by Dileep Singh, Dongming Zhu, Waltraud M. Kriven and Sanjay Mathur.


# FINITE ELEMENT MODELING OF COMPRESSOR BLADE LEADING EDGE CURL, EROSION AND DEFORMATION

George M. Slota[1] and Douglas E. Wolfe[1,2]
[1] Applied Research Laboratory, and
[2] Materials Science and Engineering Department, The Pennsylvania State University
119 Materials Research Institute
University Park, PA 16802, USA

## ABSTRACT

Leading edge curl is a deformation phenomenon that has been observed to occur on the first 250-750 microns of the leading edge of compressor blades in jet turbine aircraft. It is especially prevalent for aircraft operating in sandy or dusty environments. This deformation affects the aerodynamic properties of the blade, causing decreases in engine performance and time between required maintenance. The purpose of this work was to recreate leading edge curl using finite element methods with two and three dimensional blade models. A variety of simulation parameters were tested, including the impacting particles' diameter, velocity, and angle of impingement. The resulting blade deformations produced from these simulations were examined for their resemblance to observed curl on fielded components based off of their measured deformation shape and magnitude. From this research, it was determined that particles of 300 microns and smaller in diameter do not have sufficient energy to plastically deform the tested blade in the absence of erosion. In comparison, larger particles of about 1000 microns are capable of causing blade deformation in the absence of erosion with as few as 1-5 particle impacts. Additionally, impact angles between 30-45 degrees resulted in curl deformation most closely resembling that observed on fielded components. This research offers new insight into the leading edge curl phenomenon and provides a basis for future work in which preventative methods for curling could be simulated and tested.

## 1. INTRODUCTION

Turbojet engines operating in sandy or dusty environments are likely to intake a large number of small granular particles up to ~1000 microns or larger in diameter. A majority of this intake occurs as the aircraft creates a dust plume while landing and taking off. The intake of these particles results in significant erosion and deformation to engine components, especially to first stage compressor blades/blisks. Eroded and deformed compressor blades increase engine vibration, fuel consumption, and combustion temperatures[1]. This leads to higher maintenance costs and a shorter engine life expectancy. Erosion and other types of foreign object damage are estimated to cost in excess of four billion dollars annually[2].

As a compressor blade erodes, the leading edge decreases in thickness, and can eventually deform into a curled shape as shown in Figure 1. The horizontal and vertical magnitudes of the deformation, measured using the method shown in Figure 1, are expected to vary between 250-750 microns, depending on the service condition. This final curling magnitude is heavily dependent on the undeformed geometry of the leading edge. A thicker leading edge will require significantly more erosion to fully curl than an initially thinner one.

It has been observed that, depending on leading edge thickness, larger diameter particles can deform the leading edge without smaller particles first thinning the leading edge through erosion. The velocity and trajectories (angle and location of impact) of impacting particles have been studied, but purely in the context of erosion[3-9]. The investigation and substantiation of the possibility of curling without preliminary erosion was the primary aims of this research effort.

At present, no systematic studies exist in the literature examining the exact conditions under which curling is probable to occur. In this work, the primary objective was to simulate a broad range of particle impact conditions on the leading edge of a compressor blade and, from this, determine the approximate range of conditions needed for leading edge curl to occur. The various tested conditions included the impacting particle's diameter, velocity, and angle of impingement. From this experimentation, new insight into these conditions needed for the curling phenomenon was established. This research also determined the finite element method to be a valuable tool in assisting efforts towards examining erosion behavior and the phenomenon of leading edge curl and deformation.

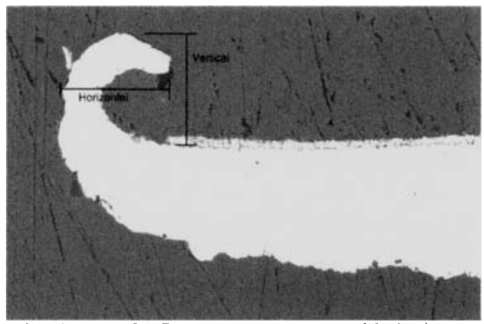


Figure 1 - The leading edge (L.E.) of a first stage compressor blade demonstrating the geometry of curling and the measurement methodology.

## 2. EXPERIMENTAL PROCEDURE

The use of finite element analysis allowed the examination of considerably more variables than could be achieved using in situ or laboratory testing, due to a higher cost effectiveness as well as a shorter turn-around time between tests. All modeling work for this effort was completed using the finite element analysis software Abaqus/Explicit v6.7-1. Abaqus/Explicit has previously been demonstrated to be a valuable tool in analyzing deformation to ductile metals due to particle impingement[2,10].

### 2.1 Model Setup

The blade models used for this work were created using two dimensional data obtained from coordinate measuring machine (CMM) measurements of an existing blade component. The blade geometry was modeled in both two and three dimensions. Only the first 4 mm back from the blade's leading edge was simulated in an effort to reduce computational costs. The two dimensional meshed model of this blade contour used in Abaqus is shown in Figure 2. The creation of a three dimensional model involved taking the base two dimensional model and extruding it about 12.7 mm into the z-axis. Different mesh densities were experimented with to determine an element size that offered the best balance between simulation accuracy and needed computation time.

The impacting particles were modeled to be circular for two dimensional modeling work and spherical for three dimensional work. The geometry of the impacting particle can have a significant impact on the resulting deformation. However, modeling different particle geometries was well beyond the scope of this effort. The particles were also modeled under the assumption that they elastically respond upon impact, but do not deform plastically or fracture. This has been observed to not always be the case, especially for high velocity impacts. Post analysis of impinging media used during in-house erosion testing has confirmed some particles do fracture after impact.

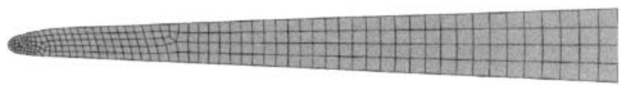

Figure 2 - Meshed model of the two dimensional "Baseline" blade.

For the two dimensional models, a 'Plane Strain' element type was used in Abaqus. This element type uses zero normal and shear strains for the third dimension under the assumption that the modeled part has a large in-plane thickness relative to the planar (x, y) dimensions. This correlates to an aircraft compressor blade as part of a blisk, which has a much longer radial length than thickness or width. For three dimensional modeling, the element type '3D Stress' was used. This element type does not make any assumptions about the stresses and strains the model will undergo during simulation. The options for element distortion control and ALE (Arbitrary Lagrangian-Eulerian) adaptive meshing were enabled for simulations where large strains resulted in mesh instability causing the simulation to end prematurely[11].

For interactions between the particle and blade the coefficient of friction was set at 0.3. Other simulation work[12] has demonstrated that the crater depth for impacting particles has a strong dependence on the frictional coefficient between 0.0 and 0.1. For values between 0.1 and 0.5 the differences in dependencies are negligible. A value of 0.3 is both physically realistic and more than suitable for the current work.

The models were designed for multiple particle impacts to occur on a single blade leading edge. The particles were aligned along the desired impacting angle and were all given the desired velocity at the beginning of the simulation. For three dimensional models, particle groups were offset along the z axis to ensure deformation occurred along the entire leading edge length. Figure 3 shows a representation for the initial (a) two and (b) three dimensional simulations.

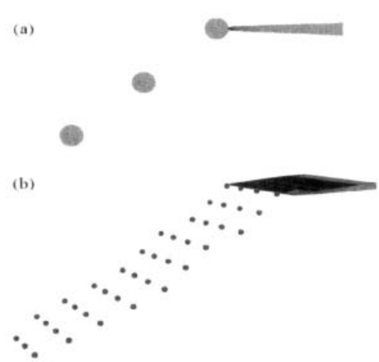


Figure 3 – Initial model setup for (a) two and (b) three dimensional simulations. Note: spacing between particles and total number of particles simulated has been reduced for demonstrative purposes.

The spacing between particles during actual testing was much larger than what is shown. The large spacing between particles allowed most elastic blade oscillations to dampen between subsequent impacts. Not allowing enough time for blade oscillations to dampen would produce a chaotic element into the model as impact locations on the leading edge would vary between different simulations. However, some models were processed with very small spacing between impacts in order to validate the possible effects that rate of impact plays in blade deformation magnitude.

## 2.2 Material Properties

The material of the baseline blade was simulated to be AM355 stainless steel alloy. AM355's yield stress and modulus were calculated from its elevated temperature curve in The Atlas of Stress-Strain Curves[13]. Other material data for AM355, including density and the Poisson's ratio, was retrieved from the ASM Handbook[14]. The material properties for the particles was assumed to be that of sedimentary rock with a Young's modulus value provided by Mark's Standard Handbook for Mechanical Engineers[15]. Previous research has shown that the type of particle (i.e., silica, quartz, alumina) will have a significant impact on the erosion behavior due to the particle geometry (spherical or irregular shape) and mechanical properties such as modulus and fracture behavior[6,7]. Table I summarizes the elastic blade material data and particle properties used in this modeling effort.

Table I. Property Definition for all Materials

| Elastic Properties of Particle and AM355 | | | Plastic Properties of AM355 | |
|---|---|---|---|---|
| | Particle | AM355 | Yield Stress in GPa | Plastic Strain |
| Young's Modulus in GPa | 103 | 162 | 1.655 | 0.0 |
| Poisson's Ratio | 0.3 | 0.3 | 1.786 | 0.000773 |
| Density in $kg/m^3$ | 2,760 | 7,910 | 12.36 | 1.719 |

The material definition for AM355 also included its plastic response. The plastic behavior for a given material is defined within Abaqus by a table of yield stresses versus plastic strains. As listed in Table I, the table of yield stresses and strains used during this testing has three rows of values. The first row defines a point at the highest applied stress immediately prior to yielding. The second row gives a point defining the initiation of yielding of the material. The third value was created for additional model stability, and was calculated based on the slope between the materials' yield stresses and the materials' ultimate tensile stresses. For stresses and strains between these points, a linear relationship is assumed. Ten percent (10%) work hardening was also assumed for this material definition.

## 2.3 Analysis of Results

There were two primary metrics used in this effort to evaluate blade deformation magnitude and geometry with relation to curling. The first metric was the average deformation of the horizontal and vertical components (X+Y)/2 and the second metric was the deformation ratio between the horizontal and vertical components. The deformation ratio was taken as the value of (X/Y) or (Y/X) that was less than 1. This was done in order to limit the possible range and ease the analysis of collected data. Neither the horizontal nor vertical deformation component is considered more important to defining curling geometry for the current effort.

The values of the horizontal and vertical deformations were retrieved from the blade models using the methodology given previously in Figure 1. Curling magnitudes measured from in-service blades have been noted to be between 250 and 750 microns for select components, with an average value close to 500 microns being common. However, these magnitudes are heavily dependent on factors such as operational environment and time on wing. A ratio between each of the deformation components should ideally be closer to one than to zero. It is difficult to define a range explicitly, as curling has been observed with large differences in the horizontal and vertical components, although values greater than ~0.2 would be considered reasonable.

## 3. THEORETICAL ANALYSIS

Because the blade model uses a fixed boundary condition at the far end from the leading edge, it is possible to use on this current model established methods for the study of cantilever beams. Analytical studies have been done to determine the exact deflection of a non-prismatic beam under a static load[16,17]. However, due to the nonuniform moment of a blade model along its length and the general complexities of modeling impulse loadings and large deformations, an exact solution for gross plastic deformation is well beyond the scope of non-numerical methods. The blade model instead will be considered as a uniform rectangular member under an impulse loading by a fixed mass in order to simplify our analysis and use available non-numerical methods[18,19]. The motivations for this analysis are twofold. It is initially hoped to establish a lower bound for particle impact velocity and mass that will result in gross deformation to the blade. It is also desired to explain the material and analytical background for the appearance and magnitude of curling due to the dynamics of the blade under high energy impact.

### 3.1 Minimum Impact Energy for Blade Deformation

For now, the blade model is to be considered a rectangular beam of mass, m, and length, L, fixed at one end. The maximum elastic bending energy that can be absorbed by the beam is given by Equation 1, where $M_o$ is the static plastic moment, E is the Young's modulus, and I is the moment of inertia for the cross section. For a rectangular cross section, I is given by $bh^3/12$, where b is the in-plane width of the model and h is the total vertical thickness. In order to establish a lower bound, the chosen h for calculation will be the blade model's minimum thickness.

$$E_B = \frac{M_o^2 L}{2EI} \tag{1}$$

The static yield moment $M_o$ can be given by Equation 2, where b and h are as previously defined and $\sigma_y$ is the yield stress. It is noted by Parkes[18] how Manjoine[20] has listed that the dynamic plastic moment can be over two times or more the static plastic moment for high strain rates. However, because this initial analysis is only currently looking for an absolute lower bound, the static value can reasonably be used.

$$M_o = \frac{bh^2}{4}\sigma_y \tag{2}$$

In order for the blade to plastically deform on impact, the kinetic energy of the impacting particle needs to be greater than the maximum elastic bending energy the blade can absorb. In other words, Equation 3 needs to be satisfied, where m is the mass of the particle and v is the particle's velocity.

$$\frac{1}{2}mv^2 \geq \frac{M_o^2 L}{2IE} \tag{3}$$

Using kinetic energy as a baseline, it can be assumed that the overall blade deformation will increase exponentially with an increasing particle velocity and/or diameter. Impacts during simulation have occurred at a variety of angles, but for now it will be assumed that impact is directly normal to the blade and is defined as an impact angle of 90 degrees. This will impart the greatest energy into the vertical deflection of the blade and continue to allow a lower bound to be established.

By using the known material properties and blade and particle dimensions, the effective minimum particle velocity needed for blade deformation can be calculated as a function of particle mass. After substitution and cancellation for I and $M_o$ in Equation 3, Equation 4 is determined, which gives the minimum necessarily impact velocity to deform the simplified blade model with respect to particle mass. Conversely, it is trivial to rearrange the terms in the equation and solve for minimum particle masses as functions of known velocities.

$$v \geq \sigma_y \sqrt{\frac{3}{4}\frac{bhL}{E}} \tag{4}$$

Using the material properties given in Table I, as well as the known model and blade parameters it is now possible to calculate lower velocity bounds for each of the tested particle sizes. Below these velocities, it is not expected that any gross plastic deformation will occur. Calculation of these values gives a further means to validate the simulation model and results. For each of the tested particle sizes (150, 300, and 1000 microns), the minimum velocity values were calculated. It was determined that these velocities are approximately 550 meters per second for the 150 micron particle, 275 meters per second for the 300 micron particle, and 83 meters per second for the 1000 micron particle. Based on these values, it can be noted that numerical simulation will likely show large plastic deformation for the largest particle size. Taking into account the fact that a larger dynamic plastic moment and moment of inertia on the actual blade model will likely increase the necessary minimum particle velocity by a factor of two or more, it does not seem likely that either of the smaller particle sizes will show much plastic deformation at any of the tested velocities for a single impact.

It is very important to note that this current modeling primarily considers the effects of particle impacts that occur singularly. This was done to ensure consistency with results across a wide range of parameters. It is an almost certainty that particles do not impact an in-service blade in an ordered or evenly spaced fashion with respect to time. The energy imparted into the blade in these circumstances would be a summation of the individual particle contributions for a given time period. A lower velocity or mass bound for these conditions value may possibly be calculated by analyzing the average particle diameter and velocity with respect to the particle intake rate and impact duration. This case is considered in the results and validation section.

3.2 Background on the Analytical Basis for Curling

Next, it is desired to use an analytical basis to explain why the blade has been observed to deform into a curled shape and a possible magnitude based on particle kinetic energy. In order to do so, the case when an impacting particle has a considerably higher kinetic energy than the minimum energy needed for the blade to deform needs to be considered. This occurs when the ratio of kinetic energy to the minimum energy, as defined as R in Equation 5, is much greater than 1.

$$R = mv^2 \frac{EI}{M_o^2 L} >> 1 \tag{5}$$

This problem was originally solved by Parkes[18], with additional insight and accuracy improvements given by Ting[17] and Symonds and Fleming[21]. Parkes's original solution will be used for this discussion for simplicity. As mentioned previously, the blade is considered to be a uniform cross-section cantilever of a rigid-plastic material with a mass, m, attached to the tip and given an initial velocity, v. Parkes determined that following the mass being given its initial velocity, the state of the blade is given by Figure 4. At any time, t, after impact, there is a plastic hinge in the blade with a moment, $M_p$. The initial location of this hinge, x, is not at the very tip but at a finite distance away, as will be explained later. The part of the beam on the side of the hinge towards the impact tip acts as a rigid body rotating around the hinge, while the part of the beam on the opposite side of the hinge is directly unaffected by the impact until it is reached by the hinge. The location of this hinge is a function of time and model parameters.

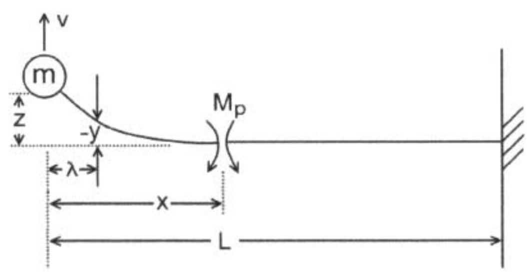


Figure 4 – The condition of the cantilever after loading. Adapted from Parkes[18].

Parkes was able to determine the final vertical displacement (-y at distance, λ, from the tip) of the cantilever for all points along its initial length. This function of displacement versus distance is given by Equation 6, where $\beta = ML/2m$ and $\xi = \lambda/L$, for varying values of particle impact energy. The final deformation of the tip, z, is the case where $\xi = 0$. There are two major components that determine the total displacement in Equation 6, which include the large local deformation near the tip of the blade, as well as the total displacement of the entire blade length due to rotation around the fixed end after the traveling hinge reaches that point and dissipates all of the remaining energy of the rotating cantilever. The local deformation near the tip can give the appearance of a distinct elbow in the displacement curve. One of Parkes's findings was that for highly dynamic impacts of an object of smaller mass than that of the cantilever, the local deformation near the tip is dominant with almost no rotational deformation around the fixed end. For impacting objects of large mass and low velocity the blade deforms in an almost straight line, all deformation being due to rotation around the fixed end. This corresponds to how almost no global rotation is observed during the current simulations of high velocity low mass particle impacts. It is also likely observed due to in part to the increasing blade thickness closer to the fixed end.

$$\frac{yM_pM}{m^2v^2} = \frac{\beta}{3(1+\beta)} - \frac{\beta\xi}{3(1+\beta\xi)} + \frac{2}{3}\ln\frac{1+\beta}{1+\beta\xi} \tag{6}$$

Through experiment, however, Parkes determined that there was one significant difference in one respect to his analytical solution. The difference was how there was a finite length of the initial tip that did not undergo any deformation. Parkes explained that an impacting object deforms upon impact, transferring a constant momentum to the tip of cantilever which corresponds to a finite force. The dynamic plastic moment is then reached at a point x away from the location of impact as given by Equation 7, where b is the width of the impacting object. Parkes gives a possible value for the initial dynamic plastic moment in this instance to be three to five times the static one.

$$x = \frac{3M_p b}{mv^2} \tag{7}$$

The elbow region mentioned previously corresponds to the region immediately after the value of x, where the dynamic plastic moment is at its greatest. The dynamic plastic moment tends to drop as the plastic hinge moves away from the tip due to rate of strain effects. We can apply knowledge of the location of the elbow region to determine an initial location away from the leading edge where the blade starts to curl. As mentioned, the cantilever shape after impact determined analytically and experimentally by Parkes closely match the results observed for a single particle impact in simulation.

Therefore, a possible estimation for curling magnitude can now be calculated based on Equation 7. In this instance an estimate for b as 250 microns is used based on an approximation of the observed maximum width of contact the 1000 micron particle maintains during impact with the blade. A value for the dynamic moment is selected to be three times the static one. Inputting these values into Equation 7 with an impact velocity of 454 meters per second results in a value of approximately 571 microns. This value is indeed very similar in magnitude to what is expected and has been observed after a single impact in blade simulation.

Figure 5 gives the result of a series of 454 meter per second 1000 micron particle impacts. From figure 5, it can be observed that there is a distinct elbow after the first impact as anticipated at a value of approximately 500 microns as predicted by Equation 7. However, subsequent impacts of large high energy particles tend to only contribute to the horizontal deformation characteristic of curling without further deformation along the blade length towards the fixed end. A possible explanation for why the blade deforms closer to the leading edge during subsequent impacts is due to the strengthening of the material at the hinge after yielding, which results in relatively lower stresses required to deform the blade away from the hinge and towards the leading edge.


Figure 5 - Progression of three impacts by a 1000 micron particle at a velocity of 454 meters per second. Note that a majority of the vertical deformation occurs after the initial impact.

The preceding analyses give estimates for the minimum energy needed for blade deformation and possible curling magnitude that could each be calculated based on known engine dynamics and environmental conditions. Applying analytical methods to calculating the deformation geometry based on particle trajectory as well as calculating the possibility for gross deformations due to simultaneous impacts are beyond the scope of this current effort, but might make for promising future work.

## 4. RESULTS AND DISCUSSION

As mentioned, a parametric study was done on a number of simulation variables, including particle diameter, particle velocity, and particle angle of impact. As is listed in Table II, particle diameters of 150, 300, and 1000 microns, particle velocities of 274, 366, 454, and 518 meters per second, and impact angles of 10, 20, 30, 37, 45, and 60 degrees were all simulated.

Table II. Tested Simulation Parameters

| | |
|---|---|
| Model Dimensionality | 2D, 3D |
| Particle Diameters | 150, 300, 1000 microns |
| Particle Velocities | 180, 274, 366, 454, and 518 meters per second |
| Impact Angles | 10, 20, 30, 37, 45, 60 degrees |

These values match the range of conditions that are considered to exist for particles impacting a first stage compressor blade. Simulations were also run with a velocity of 180 meters per second in order to match the maximum velocity produced from testing on physical blades using an in-house laboratory erosion blasting rig. It was intended for the simulated blade models to be validated against blade deformation produced from laboratory testing as well as blades that were retrieved from in-service. Overall, the results that are presented in this paper represent the culmination of the analysis of more than ten thousand simulations.

For the results shown, the two dimensional blade models were subjected to impacts from six particles except when otherwise noted, while three dimensional models were impacted with 420 particles offset along the entire length of the leading edge. These values were chosen based on preliminary work, where they were observed to be the minimal number of impacts necessary to deform the blade enough for curling at the lowest tested velocity. It should also be noted that preliminary testing with up to 20 large particle impacts also demonstrated how a larger number of impacts does not necessarily result in a higher magnitude of curling. A majority of the total and vertical deformation was observed to occur during the first few impacts, with subsequent impacts only elastically deflecting the blade while not causing additional gross plastic deformation.

4.1 Particle Diameter

The diameter of the impacting particles was observed to have a significant effect on the resulting magnitude of leading edge deformation. Table III shows the overall average of the deformation values (X+Y)/2 measured on the blades under the entire range of velocities (274-518 meter per second) and impact angles (10-60 degrees) for the given particle sizes. The values listed in Table III for the 150 and 300 micron particles contain measurements only from the two dimensional model. Similar to the results obtained on the two dimensional model and what was expected based on the analytical calculations, initial testing done on the three dimensional blade model for 150 and 300 micron particles did not yield any substantial deformation under the conditions simulated. Therefore, a full parametric study of the 150 and 300 micron particles across all angles and velocities was not performed to minimize the number of three dimensional simulations that needed to be processed.

Table III. Average Deformation vs. Particle Size and Impact Angle

| Particle Size in microns | Average Deformation in microns | | | | | |
|---|---|---|---|---|---|---|
| | Impact Angle in degrees | | | | | |
| | 10 | 20 | 30 | 37 | 45 | 60 |
| 150 | 0.65 | 4.81 | 6.74 | 5.96 | 4.90 | 1.65 |
| 300 | 2.69 | 12.4 | 17.9 | 20.1 | 12.2 | 5.09 |
| 1000 | 86.4 | 405 | 533 | 564 | 466 | 195 |

As is shown in Table III, particle diameters of 150 and 300 microns both produced minimal leading edge deformation on the two dimensional model. Subsequent testing was performed up to 20 impacts with the 150 and 300 micron particles, with negligible differences in resulting measurements. The average deformation measured for 1000 micron diameter particles fell within the 250-750 micron range previously mentioned. Overall, there was minimal difference between the average values obtained from the two dimensional and three dimensional simulations.

These results suggest that smaller particles are unable to independently cause the magnitude of deformation necessary for curling. It is possible that they contribute more towards erosion of the blade while larger particles are more likely to cause gross plastic deformation. As curling did not result from 150 and 300 micron impacts, examination of the different particle diameters' effect on the deformation ratio no measurements could be performed. Because of the lack of deformation with the smaller particles, further discussion in this paper will focus solely on simulations run with 1000 micron diameter particles.

4.2 Particle Velocity

It was observed that the magnitude of blade deformation was heavily correlated with the particle's velocity. As was noted with increasing the particle diameter, a higher initial kinetic energy of the impacting particles resulted in correspondingly greater magnitudes of blade deformation. Figure 6 shows the averages deformations (X+Y)/2 as a function of the particle velocity for 1000 micron particles in two and three dimensional simulations with impact angles between 10 and 60 degrees.

As can be observed from Figure 6, the average blade deformation increased with increasing particle velocity. Impact velocities between 274 and 518 meters per second all produced average deformations within the anticipated 250-750 micron range. A deformation magnitude necessary for curling was not observed at 180 meters per second during for the individual impacts tested.

The large spread in collected data in Figure 6 for 454 and 518 meters per second is explained by the fact that the shown values are averaged over all tested angles of particle impact. As will be examined in Section 3.3, the particle impact angle can have a significant effect on blade deformation geometry and magnitude.

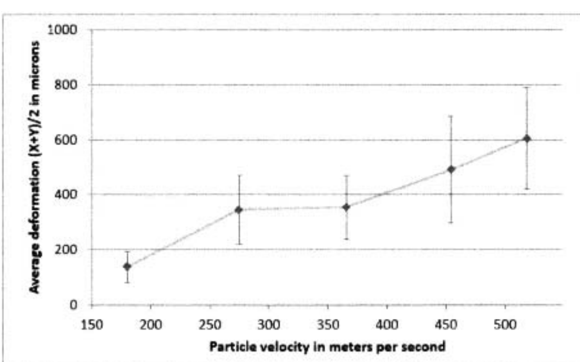


Figure 6 – Average deformation magnitude (X+Y)/2 in microns vs. particle velocity in meters per second for 1000 micron particles and impact angles between 10 and 60 degrees.

The effect that different particle velocities had on the curling geometry as defined by the deformation ratio (lesser of (X/Y) and (Y/X)) is shown in Figure 7. Figure 7 displays the averages of the deformation ratio for the tested particle velocities between 274 and 518 meters per second at angles between 10 and 60 degrees. As stated previously, values above ~0.2 are expected for proper curling geometry.

From Figure 7, it appears that impact velocities between 366 and 518 meters per second resulted in the best ratios relative to the other tested velocities. Analysis of simulations where curling has occurred show that the blade deforms vertically first before deforming horizontally into the final curl geometry. Low velocity particle impacts at certain angles appear to be able to deform the blade vertically but lack the impact energy needed to fully curl the blade horizontally.

Overall, the absolute difference in ratios between the different velocities was not very large. It is also noted that the average ratio for none of the tested velocities was above the expected 0.2 value. As previously mentioned, the angle of particle impact plays a large role in both the magnitude and geometry of blade deformation which will be demonstrated in the next section.

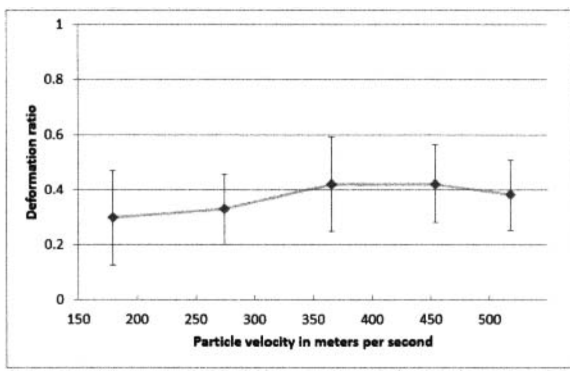


Figure 7 – Deformation ratio vs. particle veloctiy in meters per second for 1000 micron particles and impact angles between 10 and 60 degrees.

From Figure 7, it appears that impact velocities between 366 and 518 meters per second resulted in the best ratios relative to the other tested velocities. Analysis of simulations where curling has occurred show that the blade deforms vertically first before deforming horizontally into the final curl geometry. Low velocity particle impacts at certain angles appear to be able to deform the blade vertically but lack the impact energy needed to fully curl the blade horizontally.

Overall, the absolute difference in ratios between the different velocities was not very large. It is also noted that the average ratio for none of the tested velocities was above the expected 0.2 value. As previously mentioned, the angle of particle impact plays a large role in both the magnitude and geometry of blade deformation which will be demonstrated in the next section.

4.3 Particle Angle of Impact

Particles were impacted on the blade leading edge at angles between 10 and 60 degrees during testing. Prior to performing simulation work, it was suspected that curling was most likely to result at an impact angle of approximately 37 degrees. This was based on the measured geometry and known dynamics of the blades on an examined compressor blisk. The results obtained from two and three dimensional simulations appear to support this initial assumption.

A comparison of the averages of the deformations (X+Y)/2 for each angle of impact across the particle velocities of 274 to 518 meters per second is shown in Figure 8. The plot shows deformation magnitudes most similar to previously measured curling for impact angles of 20, 30, 37, and 45 degrees. The impact angle of 60 degrees also has an average value within the typical 250-750 micron range, but was on the border. In general, it appears that impact angles between 20 and 60 degrees are sufficient to cause leading edge deformation magnitudes observed in the field.

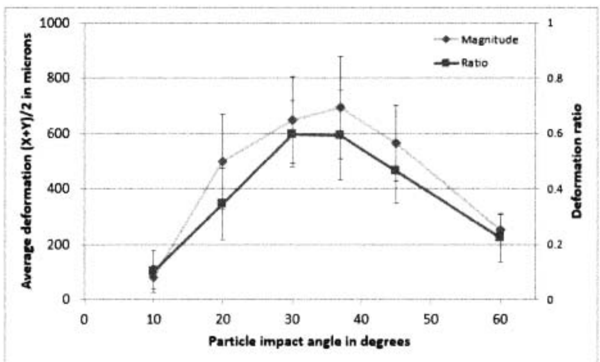


Figure 8 - Average deformation magnitude (X+Y)/2 in microns and deformation ratio vs. particle impact angle for 40 mil particles and impact velocities between 274 and 518 meters per second.

Figure 8 also shows the averages deformation ratios for all tested impact angles across the particle velocities of 274 to 518 meters per second. It is observed from Figure 8 that the highest magnitude deformation geometries as defined by the deformation ratio are for angles between 20 and 45 degrees, with the ratios at the angles of 30 and 37 degrees being highest. Based on post simulation analysis, low impact angles do not appear to be able to deform the blade vertically enough for any horizontal deformation to occur, while higher impact angles are able to deform the blade vertically but are unable to subsequently deform the blade horizontally into the final curled geometry.

The fact that both the deformation ratio and the deformation magnitude are close to the commonly measured values for curling between 30 and 45 degrees might indicate that these angles of impact are what is encountered in the field. Figure 8 also demonstrates that the deformation ratio and therefore the geometry of curling is more heavily influenced by the angle of impact rather than just the energy of impact as defined through the impacting velocity.

4.4 Model Verification and Rate of Impact

One of the most important aspects of simulation using finite element analysis is ensuring that the modeling work being performed is accurate. This can be accomplished through verifying the results of the simulations against damaged components from the field or from in-house testing. The Applied Research Laboratory's Advanced Coating Department has an in-house erosion testing rig, which allowed for adjustments to be made to some of the same impact parameters that were studied through finite element simulation for model verification. The rig included a compressed air supply which accelerates particles of multiple possible diameters to a maximum velocity dependent on the allowed air pressure. These particles strike a small blade target which can be set at variable angles. The erosion rig has flexibility in evaluating various particle types, sizes, angles of impingement, particle feed rate, and particle velocity, depending on the desired experimental set-up.

By comparing the deformation observed in fielded components to simulations and in-house tests at various impact parameters, a verification of the testing and simulating methodology was performed. Figure 9 shows results obtained from a blade removed from a blisk taken from the field, results from in house testing, our simulation results modeled using expected field conditions, and our results using the conditions present in the in-house erosion rig.

The leading edge curl deformation observed on all four images in Figure 9 is of a very similar magnitude and geometry. The curling obtained through simulation on Figure 9(c) is under the angular, velocity, and particle diameter conditions of 37 degrees, 454 meters per second, and 1000 microns. The curling shown from the in-house testing rig was obtained through 37 degrees as well, but due to the physical constraints of the rig itself, the particle velocity was much lower at only 180 meters per second. In order to validate these results, we modeled the same conditions present in the rig, which included the lower velocity, much higher impact rate, and the specific particle size distribution used. Some of the primary differences are noted below.

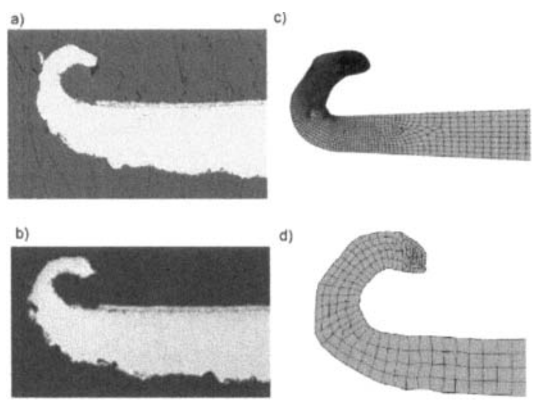


Figure 9 - (a) An optical micrograph showing the leading edge cross section of a deformed baseline blade taken from the field; (b) similar deformation of a blade that was obtained through in-house erosion rig testing; (c) two dimensional modeling simulation result produced from using field impact parameters; (d) two dimensional modeling simulation result produced from using in-house erosion rig parameters.

The particles delivered by the erosion rig are not of a uniform size or shape. The particle distribution used by the rig included a range of sizes between the smallest and largest particle diameters that were previously discussed. The particles also interact before impacting with the blade, affecting their velocity and final impact angle. This results in a much greater range of particle impact conditions experienced by the blade in this setup. The primary goal of this effort was analyzing the contribution of each impact parameter individually, which would not be possible with a simulation under these conditions.

Additionally, as was briefly touched upon in the theoretical analysis, there is a much higher rate of impact experienced in the erosion rig when compared to what was experienced in the simulations. The erosion rig delivers 100 grams of particles per minute 2.54 cm of blade width. The particle spacing necessary for simulating these conditions is considerably less than what was used previously, even for the large particles. While modeling field conditions, we allowed blade deflections to diminish before subsequent particle impacts in order to analyze the effect of individual impacts. The flow rate of the erosion rig is considerably higher than what is possible in situ, to decrease turnaround time between tests. Our analytical model and previously discussed lower velocity bounds are not directly valid in this case, as we only considered the energy of a single particle impact. To account for multiple concurrent impacts, the kinetic energy in Equation 3 would be a summation of all particles impacting the blade edge, which would therefore greatly decrease the minimum velocity given in Equation 4. Obviously, at it is not expected all particles to be of equal mass or strike the blade at precisely the same instant, a more complex relationship exists than what is given in our simplified model.

Due to the similarity in deformation magnitude and geometry as is presented in Figure 9, it is suggested that the consistent and higher rate of energy imparted onto the blade in the erosion rig is likely to have as great an effect on blade deformation magnitude as the larger but highly transient rate experienced during discrete large particle impacts. Therefore, future modeling and in house testing work should take into account not only particle velocity and magnitude, but the important role that the rate of energy transfer plays.

It should finally be noted that the velocities used for the majority of simulations, 274 to 518 meters per second, are closer to what is expected for impacts in an actual compressor section. These are the conditions that the blade in Figure 9(a) would have likely experienced. This is based on known compressor blade dynamics.

## 5. CONCLUSIONS

The primary goal for this research effort was to determine possible particle impact conditions for leading edge curl. Based on the observations made during modeling and simulation on the two and three dimensional models, a number of conclusions can be reached regarding this goal.

It was observed that small particles on the order of 150 and 300 microns in diameter do not have enough energy to cause significant plastic deformation to the baseline blade leading edge with single impacts. Even at high velocities, only minor deformation (more similar to indentation than curling) was observed. This was in line with the results obtained in the theoretical analysis. Larger diameter particles of 1000 micron were able to cause substantial deformation. It can be concluded that single particle diameters approximately 1000 microns or greater are necessary to cause gross deformations to an un-eroded blade, while smaller particles may likely contribute more towards erosion of the leading edge.

Based on the analysis of the role that the rate of impact plays on blade deformation, similar sized deformation magnitudes observed with the large particles could be obtained with the smaller particles by increasing the rate of impact at a consistent velocity to equalize the mass per unit time per unit width of impacts on the blade. Future work might consider further validating this observation by equalizing the kinetic energy of impacts while varying both the particle diameter and velocity. Further examining the rate of particle intake typically experienced in operation in the field could offer additional insights.

Particle velocities between 180 and 518 meters per second were simulated. Using 1000 micron diameter particles, deformation resembling curl was observed with velocities between 366 and 518 meters per second. The magnitude of this deformation appeared to correspondingly increase with increases in velocity. Velocities of about 454 meters per second were observed to result in the most appropriately sized curling magnitudes in the tested simulations.

A range of impact angles between 10 and 60 degrees was examined during simulation. Distinct curling geometry was most noticeable at 30, 37, and 45 degrees. Lower angles did not deform the blade vertically enough to result in appropriate curling geometry, while higher angles did not deform the blade horizontally enough to fully curl into the appropriate geometry.

Based on these simulation results, curling can occur on the baseline blade when it is subjected to single particle impacts with diameters of about 1000 microns at velocities of about 454 meters per second at an impacting angle close to 37 degrees. These results are also likely to be obtained with smaller particles or velocities at a higher rate of impact.

## 6. ACKNOWLEDGEMENTS

The authors would like to express their gratitude to the Exploratory and Foundational (E&F) Graduate Student Research Program of the Applied Research Laboratory at The Pennsylvania State University (PSU ARL) for supporting this effort. Additional support was provided by the United States Navy Manufacturing Technology (ManTech) Program, Office of Naval Research, under Navy Contract N00024-02-D-6604. Any opinions, findings, conclusions, or recommendations expressed in this material are those of the authors and do not necessarily reflect the views of the U.S. Navy.

## 7. REFERENCES

[1]T. J. Carter, Common failures in gas turbine blades, *Engineering Failure Analysis*, **12**, 237-47 (2005).

[2]X. Chen, Foreign object damage on the leading edge of a thin blade, *Mechanics of Materials*, **37**, 447-57 (2005).

[3]A. Hamed and W. Tabakoff, Experiment and Numerical Simulations of the Effects of Ingested Particles in Gas Turbine Engines, Propulsion and Energetics Panel (PEP) Symposium, Rotterdam, The Netherlands, April 1994.

[4]D. R. Nagy, V. R. Parameswaran, J. D. MacLeod, and J. P. Immarigeon, Protective Coatings for Compressor Gas Path Components, Propulsion and Energetics Panel (PEP) Symposium, Rotterdam, The Netherlands, April 1994.

[5]W. Tabakoff, Study of Single-State Axial Flow Compressor Performance Deterioration, *Wear*, **119**, 51-61 (1987).

[6]B. Borawski, J.A. Todd, J. Singh, D.E. Wolfe, The influence of ductile interlayer material on the particle erosion resistance of multilayered TiN based coatings, *Wear*, **271**, 2890-2898 (2011).

[7]B. Borawski, J. Singh, J.A. Todd, D.E. Wolfe, Multi-layer coating design architecture for optimum particulate erosion resistance, *Wear*, **271**, 2782-92 (2011).

[8]M. W. Reedy, T. J. Eden, J. K. Potter, D. E. Wolfe, Erosion performance and characterization of nanolayer (Ti,Cr)N hard coatings for gas turbine engine compressor blade applications,"*Surface & Coatings Technology*, **206**, 464-72 (2011).

[9]D. E. Wolfe, B. M. Gabriel, M. W. Reedy, Nanolayer (Ti,Cr)N coatings for hard particle erosion resistance, *Surface & Coatings Technology*, **205**, 4569-76 (2011).

[10]X. Chen and J. W. Hutchinson, Particle impact on metal substrates with an application to foreign object damage to aircraft engines, *Journal of the Mechanics and Physics of Solids*, **50**, 2669-90 (2002).

[11]ABAQUS Inc, Abaqus Analysis User's Manual, Dassault Systèmes, 2007.

[12]M. Meo, R. Vignevic, Finite element analysis of residual stress induced by shot peening process, *Advances in Engineering Software*, **34**, 569-75 (2003).

[13]Atlas of Stress-Strain Curves 2nd Edition, ASM International, Materials Park, OH, 2002.

[14]ASM International Handbook Committee, ASM Handbook Volume 19: Fatigue and Fracture, ASM International, Materials Park, OH, 1996.
[15]E.A. Avallone and T. Baumeister III, Mark's Standard Handbook for Mechanical Engineers, McGraw-Hill, 1996.
[16]S.Y. Lee, H.Y. Ke, Y.H. Kuo, Exact static deflections of a non-uniform Bernoulli-Euler beam with general elastic end restraints, *Computers & Structures*, **36**, 91-97 (1990).
[17]G. Baker, "Exact deflection in nonprismatic members," *Computers & Structures*, **61**, 515-28 (1996).
[18]E. W. Parkes, The permanent deformation of a cantilever struck transversely at its tip, *Proceedings of the Royal Society of London, Series A, Mathematical and Physical Sciences*, **228**, 462-76 (1955).
[19]T.C.T. Ting, Large deformation of a rigid, ideally plastic cantilever beam, *Journal of Applied Mechanics*, **32**, 295-302 (1965).
[20]M.J. Manjoine, Influence of rate of strain and temperature on yield stresses of mild steel, *Journal of Applied Mechanics*, **11**, 211-18 (1944).
[21]P.S. Symonds, W.T. Fleming, Parkes revisited: on rigid-plastic and elastic-plastic dynamic structural analysis, *International Journal of Impact Engineering*, **2**, 1-36 (1984).